Chemical Engineering & Processing: Process Intensification 166 (2021) 108464

Contents lists available at ScienceDirect

Chemical Engineering and Processing - Process Intensification

journal homepage: www.elsevier.com/locate/cep

CO_2 removal using 1DMA2P solvent via membrane technology: Rate based modeling and sensitivity analysis

Majid Saidi [a,*], Ebrahim Balaghi Inaloo [b]

[a] School of Chemistry, College of Science, University of Tehran, PO Box 14155–6455, Tehran, Iran
[b] School of Chemistry, Alborz Campus, University of Tehran, PO Box 14155–6455, Tehran, Iran

ARTICLE INFO

Keywords:
Absorption
1DMA2P
HFMC
Mass transfer rate
Kinetic modeling

ABSTRACT

A numerically solved reaction rate/kinetic model for CO_2 removal from a CO_2/N_2 gas mixture into novel reactive 1-dimethylamino-2-propanol (1DMA2P) solution in a gas–liquid membrane contactor was constructed. The model is assembled by considering the main transport phenomena and all possible reactions. The validated model was applied to investigate the transport phenomena in the different sides of membrane. The impact of main operation parameters on the performance of HFMC were evaluated. The influence of co- and counter-current operational modes on the absorption process was analyzed. The sensitivity analysis under moderate conditions indicated that the mass transfer resistance of gas phase is dominant with respect to liquid phase. Enhancing the liquid temperature, solvent circulation velocity, 1DMA2P concentration and also decreasing gas stream velocity increase the CO_2 absorption. The CO_2 removal using conventional and alternative amines were analyzed and compared. It is observed that due to high capacity of 1DMA2P for CO_2 capture and its low regeneration heat, it could be considered as one of the efficient solvent for CO_2 removal.

1. Introduction

Extensive efforts have been performed to solve environmental problems related to climate change and global warming [1–3]. The world is imposed to upgrade environmental strategies and applied efficient technologies that will reduce the greenhouse gas emissions into the atmosphere [4]. One of the main concerns for the future decades is mitigation of CO_2 emissions as the largest contributor to greenhouse pollution. Post–combustion CO_2 capture via chemical absorption process is a favorable method for carbon capture and storage (CCS). Amine solvents are usually used for this process since they represent high capture efficiency and selectivity towards CO_2, low energy requirement for regeneration, low degradation rate, and low corrosiveness. Different amine–based solvents have been widely used for CO_2 capture. Alkanolamine solvents can be categorized into three main groups, including primary, secondary and tertiary amines. Although, because of faster reaction rates of primary and secondary amines with CO_2, they are extensively used, but also their use has been recently limited because of their low CO_2 absorption capacity, solvent degradation and corrosion, high regeneration energy and cost. On the other hand, the tertiary amines represent higher absorption capacity, lower regeneration heat, as well as slower reaction rate. The tertiary amines catalyze the hydrolysis of CO_2 to bicarbonate without any direct reaction with CO_2. The superiority of lower energy consumption during regeneration of tertiary amines can provide the wide–spread employment of amine solvents. In recent years, the development of more efficient tertiary amine solvents has attracted extensive attention in the research community to provide a cost effective system. Currently, 1–dimethylamino–2–propanol (1DMA2P), a tertiary alkanolamine, introduced as an applicable solvent for large-scale use in bulk CO_2 absorption. The previous investigations confirmed that 1DMA2P represents better mass transfer performance and higher kinetics of CO_2 removal than the most common tertiary amines [5]. Liang *et al.* [5] investigated the CO_2 removal performance of aqueous 1DMA2P in terms of CO_2 absorption rate, CO_2 absorption heat, CO_2 equilibrium solubility, and mass transfer efficiency. Their reported results indicated that the equilibrium solubility of 1DAM2P solvent is greater than that of conventional amines such as MEA and MDEA. Kadiwala *et al.* [6] reported that 1DMA2P represents faster kinetics of CO_2 absorption compared to that of MDEA. Afkhamipour *et al.* [7] experimentally and theoretically calculated the physical properties of 1DMA2P solution such as CO_2 equilibrium solubility, density and viscosity. Liu *et al.* [8] determined the CO_2 solubility and absorption heat into 1DMA2P. They inferred that the CO_2 equilibrium solubility into

* Corresponding author.
E-mail addresses: majid.saidi@khayam.ut.ac.ir, majid.saidi@ut.ac.ir (M. Saidi).

https://doi.org/10.1016/j.cep.2021.108464
Received 3 March 2020; Received in revised form 23 March 2021; Accepted 30 April 2021
Available online 10 June 2021

Nomenclatures

C	Concentration (mol m^{-3})
C_0	Initial concentration (mol m^{-3})
C_{CO_2e}	Equilibrium CO_2 concentration in the bulk of liquid (kmol m^{-3})
$C_{CO_2-membrane}$	CO_2 concentration in the membrane (mol m^{-3})
$C_{CO_2-shell}$	CO_2 concentration in the shell side (mol m^{-3})
C_{CO_2-tube}	CO_2 concentration in the tube (mol m^{-3})
C_p	Specific heat (J mol^{-1} K^{-1})
$D_{CO_2-membrane}$	Diffusion coefficient of CO_2 in the membrane (m^2 s^{-1})
$D_{CO_2-shell}$	Diffusion coefficient of CO_2 in the membrane (m^2 s^{-1})
D_{CO_2-tube}	Diffusion coefficient of CO_2 in the tube (m^2 s^{-1})
D_{w,co_2}	Diffusion coefficient of CO_2 in pure water (m^2 s^{-1})
H	Solubility of carbon dioxide in solution (kmol atm^{-1} m^{-3})
H	Henry's constant
$k_{(R-1)}$	Forward rate constant of reaction (R−1) ($m^3 kmol^{-1} s^{-1}$)
$k_{-(R-1)}$	Backward rate constant of reaction (R−1) ($m^3 kmol^{-1} s^{-1}$)
$k_{(R-2)}$	Forward rate constant of reaction (R−2) ($m^3 kmol^{-1} s^{-1}$)
$k_{-(R-2)}$	Backward rate constant of reaction (R−2) (s^{-1})
K_i	Chemical equilibrium constant for reaction i
K_w	Chemical equilibrium constant for reaction (R−5)
L	Length of fiber (m)
m	Physical solubility (dimensionless)
N	Molar flux
n	Number of fibers
Q_g	gas volume flow rate (mL min^{-1})
Q_l	liquid volume flow rate (mL min^{-1})
r_1	Inner tube radius (m)
r_2	Outer tube radius (m)
R	Inner shell radius (m)
T	Temperature (K)
V	Velocity (m s^{-1})
$V_{z,shell}$	Velocity in the shell side (m s^{-1})
$V_{z,tube}$	Velocity in the tube side (m s^{-1})
Z	Height of the membrane contactor (m)

Greek symbols

ε	Porosity
ρ_G	Gas phase density ($kg\,m^{-3}$)
ρ_L	Liquid phase density ($kg\,m^{-3}$)
$\sigma_{CO_2-N_2}$	Lennardejones parameter (A)
χ	Thermal conductivity (Wm^{-1} K^{-1})
μ	Viscosity (Pa.s)
Ω	Collision integrals
ΔH_i	Heat of absorption (J mol^{-1})

1DMA2P solution reduces as both reaction temperature and solvent concentration increases, and the CO_2 solubility enhances as the CO_2 partial pressure increases.

Gas-liquid absorption process is conventionally performed using sprayer, bubble, plated and packed columns, but the main challenge in designing and operating these columns is to intensify the mass transfer rate by providing as much contact area as possible. Another important drawback of these columns is the interdependence of the two fluid phases to be directly contacted, which may lead to problems such as foaming, flooding, emulsions and unloading. An alternative approach to overcome these disadvantages and provide substantially more contact area than conventional methods is non–dispersive contact via a membrane. Recently, hollow fiber membrane contactors (HFMC) are introduced as one of the most promising alternative to intensify the CO_2 removal by chemical absorption. The main advantage of HFMC is to make use of permeable membrane to enhance chemical absorption with equilibrium–limited chemical reactions. Also, since two fluid streams are independent in the HFMC, the available contact area remains unchanged at various flow rates. Indeed, the membrane acts as a physical barrier and allows non–dispersive gas–liquid contact. Moreover, membrane contactors present flexibility, modularity, compact size, high contact area, easy installation and low cost.

HFMC has been extensively considered both theoretically and experimentally, and interesting results have been achieved in terms of CO_2 removal from the flue gases. Cao et al. [9] studied the CO_2 removal by aqueous 1DMA2P solution in a polytetrafluoroethene HFMC. Their reported results indicated that the enhancement of amine temperature and concentration will improve the CO_2 removal efficiency. Experimental investigation by deMontigny et al. [10] showed that the overall mass transfer coefficient (K_Ga_v) in membrane contactor is significantly greater than that in the packed tower. Rangwala [11] studied and compared the CO_2 absorption into different solvent via traditional packed column and membrane module. They observed that the K_Ga_v in HFMC can be 3–9 times greater than traditional packed column. Iliuta et al. [12] concluded that under the same specific surface area and volume, the HFMCs has a higher CO_2 removal efficiency to the packed column. Also, they inferred that the CO_2 absorption can be significantly intensified with an enhancement in the specific area of membrane module. More detailed literature review is presented by Saidi et al. [13, 14], Luis et al. [15], Cui and deMontigny [16], and Hillal and Ismail [17].

In this research, a two–dimensional reaction rate/kinetics model is developed to assess and analyze the CO_2 removal using aqueous 1DMA2P solution functioning under industrial relevant operating conditions. The intensification potential of the aqueous 1DMA2P solution for CO_2 absorption by application of a polypropylene HFMC is estimated and validated in comparison with other solvents such as monoethanolamine (MEA), diethanolamine (DEA), methyldiethanolamine (MDEA), piperazine (PZ) and 4-(diethylamino)-2-butanol (DEAB) solutions. Also, the impact of essential parameters on the CO_2 removal have been determined.

2. Gas-liquid absorption by membrane technology

In the membrane separation technology which considered in the present work, the gas and liquid streams pass through independent parts of contactor with independent flow rates and counter–current operation mode. Module inner diameter (R) is 63.50 mm and total number of fibers are 3600. The gas stream enters a shell with a diameter of 0.529 mm at a pressure of 200 kPa and a velocity of 1 mm/s and the liquid stream enters a tube with an internal diameter of 0.22 mm. Module have 3600 fiber with porosity of 25%. As conceptually illustrated in Fig. 1, the CO_2 molecules as the reactive species moves from the gas phase to the external surface of the membrane and then diffuses into the membrane. Finally, the CO_2 molecules are chemically absorbed by aqueous 1DMA2P solution where they react. In the following, a stripper is used to extract the CO_2 molecules from the rich liquid solution and the regenerated solvent is recycled to the absorber.

3. Kinetic investigation

Donaldson and Nguyen [18] developed a base-catalyzed hydration mechanism for CO_2 absorption in tertiary amine solutions. According to this mechanism, the tertiary amines catalyze the hydration reaction of CO_2. The reaction mechanism between CO_2 and aqueous 1DMA2P solution and also, required kinetic and equilibrium data are as follows [5,

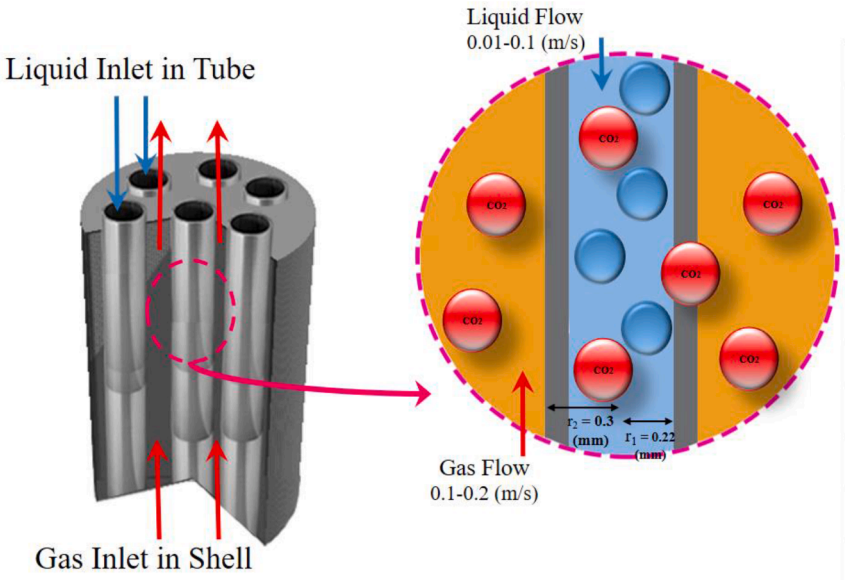

Inner Tube Diameter, r_1 [mm]	0.22
Outer Tube Diameter, r_2 [mm]	0.30
Module inner Diameter, R [mm]	63.50
Total Number of Fibers [−]	3600
Fiber Porosity, ε [%]	25
Inner Shell Diameter, d [mm]	0.529
Module Length, L [m]	0.25
Temperature, T [K]	298–318
Gas Inlet Pressure, P [kPa]	200
Gas Velocity, U_g [m s−1]	0.01–0.20
Liquid Velocity, U_l [m s−1]	0.01–0.10

Fig. 1. Schematic of HFMC.

6,19–22]:

$$CO_2 + 1DMA2P \overset{K_{R-1}}{\leftrightarrow} 1DMA2PH^+ + HCO_3^- \quad \text{(R-1)}$$

$$CO_2 + OH^- \overset{K_{R-2}}{\leftrightarrow} HCO_3^- \quad \text{(R-2)}$$

$$1DMA2P + H^+ \overset{K_{R-1}}{\leftrightarrow} 1DMA2PH^+ \quad \text{(R-3)}$$

$$CO_2 + H_2O \overset{K_{R-4}}{\leftrightarrow} H^+ + HCO_3^- \quad \text{(R-4)}$$

$$HCO_3^- \overset{K_{R-5}}{\leftrightarrow} H^+ + CO_3^{-2} \quad \text{(R-5)}$$

$$H_2O \overset{K_{(R-6)}}{\leftrightarrow} H^+ + OH^- \quad \text{(R-6)}$$

The K for each reactions are:

$$K_{(R-1)} = \frac{[1DMA2PH^+][HCO_3^-]}{[CO_2][1DMA2P]} \quad (1)$$

$$K_{(R-2)} = \frac{[HCO_3^-]}{[CO_2][OH^-]} \quad (2)$$

$$K_{(R-3)} = \frac{[1DMA2PH^+]}{[1DMA2P][H^+]} \quad (3)$$

$$K_{(R-4)} = \frac{[H^+][HCO_3^-]}{[CO_2]} \quad (4)$$

$$K_{(R-5)} = \frac{[H^+][CO_3^{2-}]}{[HCO_3^-]} \quad (5)$$

$$K_{(R-6)} = [H^+][OH^-] \quad (6)$$

All reactions are at equilibrium condition, so:

$$k_{(R-1)}[CO_2][1DMA2P] = k_{-(R-1)}[1DMA2PH^+][HCO_3^-] \quad (7)$$

$$k_{(R-2)}[OH^-][CO_2]_e = k_{-(R-2)}[HCO_3^-] \quad (8)$$

The temperature dependency of the equilibrium constants are expressed by the following relation [19–21].

$$K_{(R-1)} = \exp\left(3.72 \times 10^9 + \frac{3.31 \times 10^7}{T} + \frac{9.38 \times 10^3}{T^2} + \frac{89.7}{T^3}\right) \quad (9)$$

$$K_{(R-2)} = \frac{K_{R-4}}{K_{R-3}.K_{R-6}} \quad (10)$$

$$K_{(R-3)} = -7.108 - \frac{-4390}{T} \quad (11)$$

$$K_{(R-4)} = \exp\left(-2.48818 \times 10^2 + \frac{2.98253 \times 10^5}{T} - \frac{1.48528 \times 10^8}{T^2} + \frac{3.32647 \times 10^{10}}{T^3} - \frac{2.82393 \times 10^{12}}{T^4}\right) \quad (12)$$

$$K_{(R-5)} = \exp\left(-2.9474 \times 10^2 + \frac{3.64385 \times 10^5}{T} - \frac{1.84158 \times 10^8}{T^2} + \frac{4.15793 \times 10^{10}}{T^3} - \frac{3.54291 \times 10^{12}}{T^4}\right) \quad (13)$$

$$K_{(R-6)} = \exp\left(3.95554 \times 10^{1} - \frac{9.879 \times 10^{4}}{T} + \frac{5.68828 \times 10^{7}}{T^{2}} - \frac{1.464561 \times 10^{10}}{T^{3}} + \frac{1.36146 \times 10^{12}}{T^{4}}\right) \quad (14)$$

Since the proton transfer reactions including (R-3) to (R-5) are reversible and instantaneous compared to mass transfer phenomenon, (R-1) and (R-2) are reasonably considered as the main rate limiting reactions.. The overall absorption rate is determined as follow:

$$r_{total} = r_1 + r_2 = (k_1 + k_2)([CO_2] - [CO_2]_e) = k([CO_2] - [CO_2]_e) \quad (15)$$

$$k = k_{(R-1)}[1DMA2P] + k_{(R-2)}[OH^-] \quad (16)$$

In the current study, the Kent and Eisenberg model [19] is used to estimate the solubility of CO_2 in the aqueous amine systems.

4. Model development

The CO_2/N_2 gas mixture (20 vol.% / 80 vol.%) enters the shell side of the contactor, while 1DMA2P solution flows through the tube side, in co- or counter-current operational modes. The mathematical model is assembled for non−wetted membrane mode on the following assumptions: steady state condition, ideal behaviors of gas mixture, laminar flow in the shell and tube sides, fully developed velocity profile in the shell and tube sides of HFMC. The material balance equations on different sections of HFMC are formulated as:

$$-\left(\frac{1}{r}\frac{\partial(r(C_iV)_r)}{\partial r} + \frac{1}{r}\frac{\partial(C_iV)_\theta}{\partial\theta} + \frac{\partial(C_iV)_z}{\partial z}\right) - \left(\frac{1}{r}\frac{(r(\partial J_i)_r)}{\partial r} + \frac{1}{r}\frac{(\partial J_i)_\theta}{\partial\theta} + \frac{(\partial J_i)_z}{\partial z}\right) + R_i = 0 \quad (17)$$

where J_i, V, t, C and R_i are the order of diffusive flux, velocity, time, concentration and reaction rate for every component, respectively. By considering the above mentioned assumptions, the governing equations in the membrane section, tube and shell sides are summarized in Table 1.

Molecular diffusion without any chemical reaction is the dominant mass transfer mechanism in the membrane side. The diffusion coefficient in the membrane section, D_{kCO2} can be calculated as [14]:

$$D_{K_{CO_2}} = 0.485 d_p \left(\frac{T}{M}\right)^{\frac{1}{2}} \quad (18)$$

For 1DMA2P solution in the tube side, $D_{CO2,\ tube}$ is determined as [23]:

$$D_{CO_2,tube} = D_{CO_2-water}\left(\frac{\mu_{H_2O}}{\mu_{1DMA2P}}\right)^{0.8} \quad (19)$$

And $D_{CO2\text{-}water}$ is given by [24,25]:

$$D_{CO_2-water} = 2.35 \times 10^{-6}\exp\left(\frac{-2119}{T}\right) \quad (20)$$

Also, the diffusion coefficient in the shell side, $D_{CO2,\ shell}$ is expressed as [26,27]:

$$D_{CO_2-shell} = 1.8583 \times 10^{-7}\sqrt{T^3\left(\frac{1}{M_{CO_2}} + \frac{1}{M_{N_2}}\right)\frac{101.325}{P\sigma^2_{CO_2-N_2}\Omega}} \quad (21)$$

The set of governing partial differential equations are solved simultaneously by application of implicit finite element method. Due to different order of magnitude between r and z directions, a scaling factor of 800 is applied in the z direction of contactor. The boundary conditions for solving the governing equations of the shell, tube and membrane sides are listed in Table 1. The convergence criterion is based on a tolerance function which considered to be less than 10−6.

$$Tolerance = \frac{\sum_{i=1}^{n}|\varphi^{i+1} - \varphi^{i}|}{\sum_{i=1}^{n}|\varphi^{i+1}|} \langle 10^{-6} \quad (22)$$

In the above equation, Φ, i and n are the decision variable (CO_2 absorption flux), the number of iterations and the number of grid points in the z direction, respectively.

5. Results and discussion

5.1. Model validation

Due to limited investigations about 1DMA2P solvent, the model is

Table 1
Governing equations and related boundary conditions.

		Governing equation	Boundary conditions
Tube side	Mass balance	$D^{nf}_{i,tube}\left[\frac{\partial^2 C_{i,tube}}{\partial r^2} + \frac{1}{r}\frac{\partial C_{i,tube}}{\partial r} + \frac{\partial^2 C_{i,tube}}{\partial z^2}\right] + R_i = V_{z,tube}\frac{\partial C_{i,tube}}{\partial z} + \frac{k_p a_p}{1-\Phi}(C_{i,tube} - C_S)V_{z,tube} = 2\langle V\rangle\left[1 - \left(\frac{r}{r_1}\right)^2\right]$	$at\ z{=}0{:}\ C_{CO_2,tube} = 0,\ C_{absorbent} = C_{in} at\ z{=}L{:}\ N_i = C_iV_{z,tube}\ at\ r{=}r_1{:}C_{CO_2,tube} = mC_{CO_2,membrane},\ \frac{\partial C_{absorbent}}{\partial r} = 0\ at\ r{=}0{:}\ \frac{\partial C_{CO_2,tube}}{\partial r} = 0,\ \frac{\partial C_{absorbent}}{\partial r} = 0$
	Energy balance	$\chi^{nf}_L\left[\frac{1}{r}\frac{\partial}{\partial r}\left(r\frac{\partial T_L}{\partial r}\right) + \frac{\partial^2 T_L}{\partial z^2}\right] + R_i\Delta H_i = \rho^{nf}_L C^{nf}_{P_L} V^{nf}_L \frac{\partial T_L}{\partial z}$	$at\ z{=}0{:}\ T_L = T^{inlet}_L,\ at\ z{=}L{:}\ \frac{\partial T_L}{\partial z} = 0 at\ r{=}r_1{:}\ T_L = T_M,\ at\ r{=}0{:}\ \frac{\partial T_L}{\partial r} = 0$
Membrane section	Mass balance	$D_{CO_2,membrane}\left[\frac{\partial^2 C_{CO_2,membrane}}{\partial r^2} + \frac{1}{r}\frac{\partial C_{CO_2,membrane}}{\partial r} + \frac{\partial^2 C_{CO_2,membrane}}{\partial z^2}\right] = 0$	$at\ z{=}0\ and\ z{=}L{:}\ \nabla C_{CO_2,membrane} = 0 at\ r{=}r_2{:}\ C_{CO_2,membrane} = C_{CO_2,shell} at\ C_{CO_2,membrane} = \frac{C_{CO_2,tube}}{m}\ where\ r{=}r_1{:}\ m = \frac{1}{h} = RT/\left(2.82 \times 10^6\exp\left(-\frac{2044}{T}\right)\right)$
	Energy balance	$\chi_{M,eff}\left[\frac{1}{r}\frac{\partial}{\partial r}\left(r\frac{\partial T_M}{\partial r}\right) + \frac{\partial^2 T_M}{\partial z^2}\right] = 0,\quad where\ \lambda_{M,eff} = \lambda_M(1-\varepsilon) + \lambda_G\varepsilon$	$at\ z{=}0\ and\ z{=}L{:}\ \frac{\partial T_M}{\partial Z} = 0 at\ r{=}r_2{:}\ T_M = T_G,\ at\ r{=}r_1{:}\ T_L = T_M$

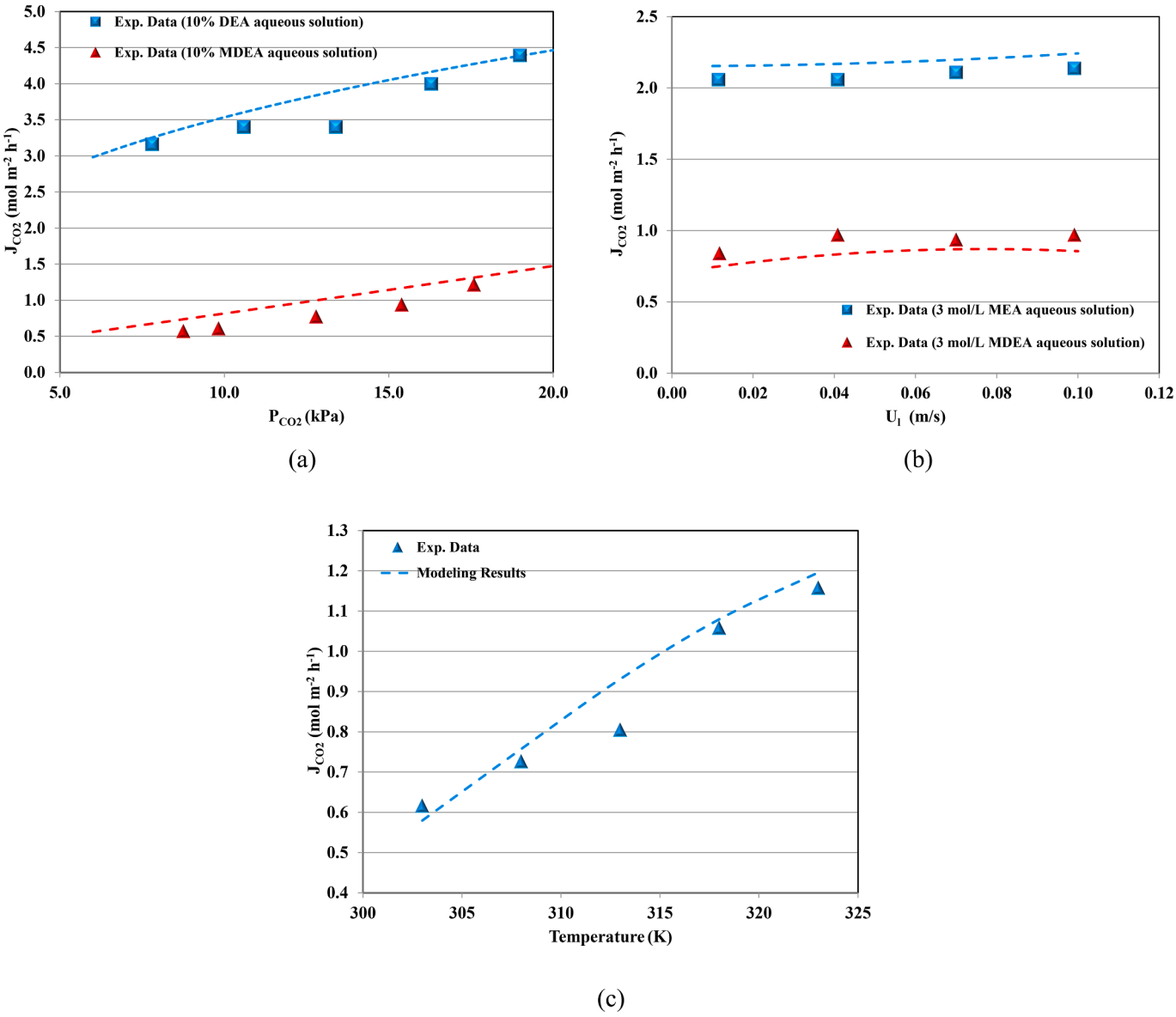

Fig. 2. Model validation, (a) CO_2 flux versus CO_2 partial pressure at T= 294 K, $U_l = 0.011$ m/s and $U_g = 0.1$ m/s [28], (b) CO_2 flux versus solvent circulation velocity at U_g=0.211 m/s; T_g: 298 K; CO_2 volume fraction in feed gas: 14 vol.% and T_l: 308 K) [29], and (c). CO_2 flux versus liquid (MDEA solvent) temperature at U_g: 0.211 m/s; T_g: 298 K; CO_2 volume fraction in feed gas: 14 vol.%; U_l: 0.0503 m/s [29].

validated with reported experimental data on CO_2 removal using common industrial solution such as MEA, DEA and MDEA [28,29]. Fig. 2-a illustrates the CO_2 absorption flux from a gas mixture of CO_2 and N_2 into DEA and MDEA solutions versus CO_2 partial pressure at atmospheric pressure. Comparison of reported results in this figure confirms that the deviation of model predicted results from the experimental data is acceptable [28]. Also, for more consideration in Fig. 2-b and c, the CO_2 absorption flux as a function of liquid velocities and temperature are evaluated based on reported experimental data [29]. The results represent that the current developed model satisfies the experimental data.

5.2. Effect of solvent circulation velocity

In the case of CO_2 absorption via HFMC, the solvent circulation velocity is believed to be one of the core factors defining efficiency of CO_2 absorption. As the velocity increases, the thickness of the mass transfer boundary layer decreases and then the concentration gradient increases. As a result, the diffusion increases. Also, the amount of available free 1DMA2P molecules increases with enhancing the solvent circulation velocity and subsequently, improves the mass transfer coefficient. The effect of solvent circulation velocity on the CO_2 removal in the HFMC is considered at different velocities in the range of 0.01–0.1 m/s and constant gas velocity of 0.1 m/s. As illustrated in Fig. 3, the CO_2 removal improves gradually with increasing the solvent circulation velocity which can be attributed to the effect of convection term on the mass transfer equation (Eq. 3). As the solvent flows with higher velocity in the tube side, the CO_2 concentration at the inner surface of the fiber decreases and as a result, a higher concentration gradient will be formed at the interface and higher CO_2 absorption will be achieved. In particular, increasing the solvent circulation velocity from 0.01 to 0.1 m/s at gas stream velocity of 0.1 m/s, temperature of 303 K and 1DMA2P concentration of 2 M enhances the CO_2 absorption approximately from 50% to 88%. But as illustrated in this figure, due to high absorption rate and capacity of 1DMA2P solvents, the effect of solvent circulation velocity on the CO_2 removal at lower velocities is more severe than higher values. Comparison of different operating temperatures in Fig. 3 reveals that although the CO_2 solubility is limited at elevated temperatures,

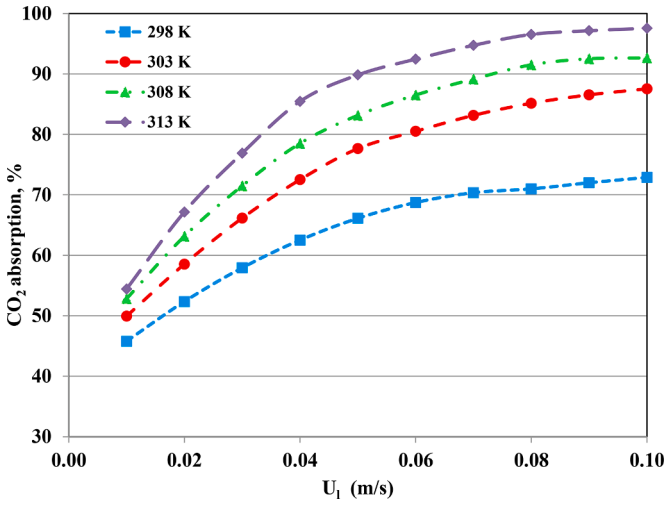

Fig. 3. CO_2 absorption flux versus liquid velocity at $C_{absorbent}$ =2 M, P_{total} = 120 kPa, Ug = 0.1 (m/s) and 3600 number of fibers.

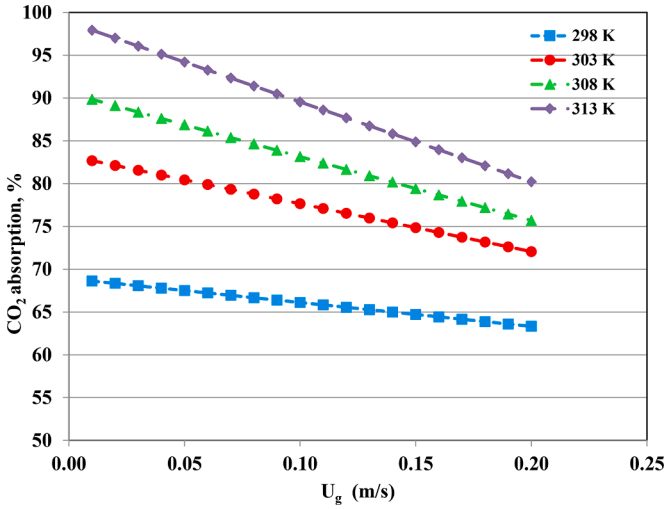

Fig. 4. CO_2 absorption flux versus gas velocity at $C_{absorbent}$ =2 M, P_{total} = 120 kPa, U_l = 0.05 (m/s) and 3600 number of fibers.

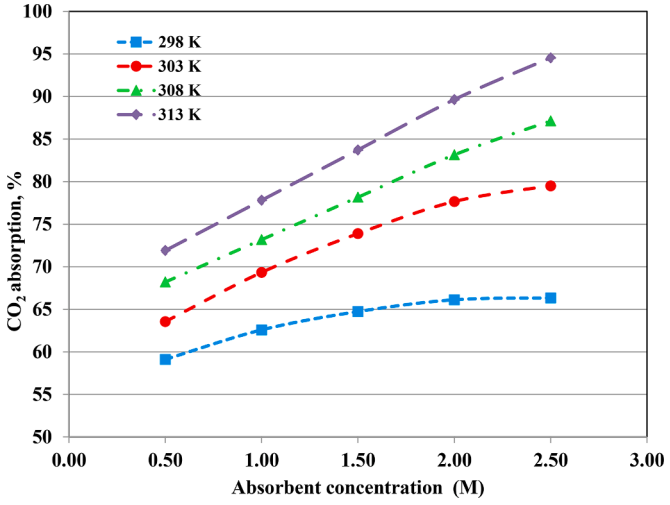

Fig. 5. CO_2 absorption percentage versus absorbent concentration at U_g = 0.1 m/s, U_l =0.05 (m/s), P_{total} = 120 kPa and 3600 number of fibers.

increasing temperature enhances the reaction rate and diffusion coefficients, leads to more CO_2 removal. For example, increasing the temperature from 298 K to 313 K at solvent circulation velocity of 0.05 m/s, gas velocity of 0.1 m/s and 1DMA2P concentration of 2 M improves the CO_2 removal from 66% to 98%.

5.3. Effect of gas stream velocity

The effect of gas stream velocity on the amount of CO_2 removal using 1DMA2P in HFMC is investigated in Fig. 4. It is well documented that enhancing the gas stream velocity reduces the residence time of gas phase in the shell side of HFMC, and as a results, it decreases the CO_2 absorption by amine solution. According to reported results in Fig. 4, the CO_2 absorption decreases continuously with increasing the gas velocity, but the decreasing trend at higher temperatures is sharper than lower temperatures. In particular, by increasing the gas velocity from 0.01 to 0.2 m/s at solvent circulation velocity of 0.05 m/s and 298 K, the CO_2 absorption reduces about 6% whereas it decrease about 18% at 313 K. Since chemical reaction takes place in the liquid phase, the mass transfer resistance in this phase is much lower than the resistance in the gas phase. Indeed, the gas phase is the controlling phase, because the major resistance is located on it. As a result, to improve the mass transfer rate, the gas stream velocity should be optimized.

5.4. Effect of absorbent concentration

Absorbent concentration is one of the most effective parameters on the CO_2 removal process and the amount of circulating solvent. The impact of 1DMA2P concentration on the removal percentage of CO_2 in the HFMC is presented in Fig. 5. The removal percentage of CO_2 increases as the 1DMA2P concentration enhances over the concentration range of 0.5–2.5 M. At the higher 1DMA2P concentrations, the more reactive 1DMA2P molecules are available for absorbing CO_2, which provides a better mass transfer performance and higher reaction rate. At lower 1DMA2P concentrations, the impact of concentration on the removal percentage of CO_2 is more considerable than higher concentrations which is related to faster reach to equilibrium condition. In addition, it was found that the CO_2 absorption will improve as temperature increases over a temperature range of 298–313 K. It can be implied from this observation that the mass transfer performance and reaction rates improve as temperature enhances. Fig. 5 indicates that an increase in the absorbent concentration from 0.5 to 2.5 M at 303 K resulted in an increment in the removal percentage of CO_2 from 64% to

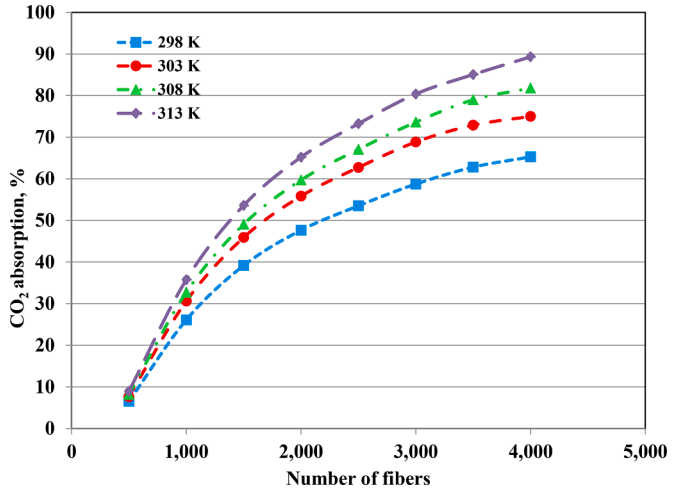

Fig. 6. CO_2 absorption percentage versus the number of fibers in the non-wetting mode at U_g = 0.1 m/s, U_l =0.05 (m/s), $C_{absorbent}$ =2 M and P_{total} = 120 kPa.

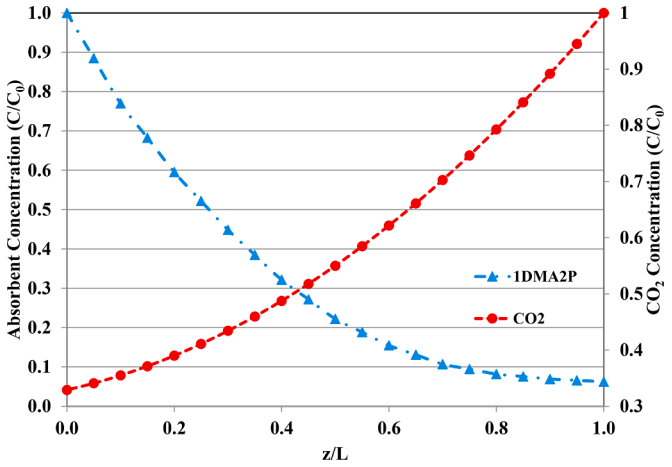

Fig. 7. CO_2 and absorbent concentration profile along the HFMC at T = 298 K, U_g = 0.1 m/s, U_l =0.05 (m/s), P = 120 kPa, $C_{absorbent}$ = 1 M and 3600 number of fibers.

80%. But it is necessary to mention that increasing the absorbent concentration would increase the solvent regeneration energy. Furthermore, increasing the 1DMA2P concentration enhances the solution viscosity. This phenomenon has negative effect on the CO_2 diffusion from the gas mixture to the liquid solvent and as a result, decreases the mass transfer coefficient. Considering the predicted results at 298 K confirms that increasing the 1DMA2P concentration more than 1.5 M has not significant positive influence on the CO_2 absorption, but at higher temperature which leads to lower solvent viscosity, the effect of 1DMA2P concentration is more considerable. High concentration of 1DMA2P will lead to other potential drawbacks, such as equipment corrosion, solvent degradation and high cost of solvent. Therefore, it is inferred that a justified absorbent concentration should be determined in designing the CO_2 removal process.

5.5. Effect of number of fibers

The variation of CO_2 absorption percentage with the number of fibers at gas stream velocity of 0.1 m/s, solvent circulation velocity of 0.05 m/s and different operating temperatures is presented in Fig. 6. The effect of number of fibers on the absorption efficiency can be considered from two points of view. First, the contact area is enhanced by increasing the number of fibers, and subsequently the CO_2 absorption will also increase. The results obviously confirm that increasing the number of fibers used in a module from 500 to 3000 at 303 K, gradually improves the CO_2 absorption from 8% to 69%. From the second point of view, an increase in the number of fibers in a module leads to decrease in the total cross-sectional area of the shell and, in turn, an increase in the volumetric gas flow rates. Therefore, by enhancing the number of fibers, the gas velocity inside the shell enhances and the CO_2 removal will mitigate. As represented in this figure, at low number of fibers, the positive effect of increasing the number of fibers is dominant and the CO_2 absorption into the 1DMA2P solution enhances sharply with increasing the number of fibers, but by intensifying the negative effect at high number of fibers, the increasing trend reduces. As illustrated in Fig. 6, increasing the number of fibers more than a certain value (3000) has not considerable influence on the CO_2 removal.

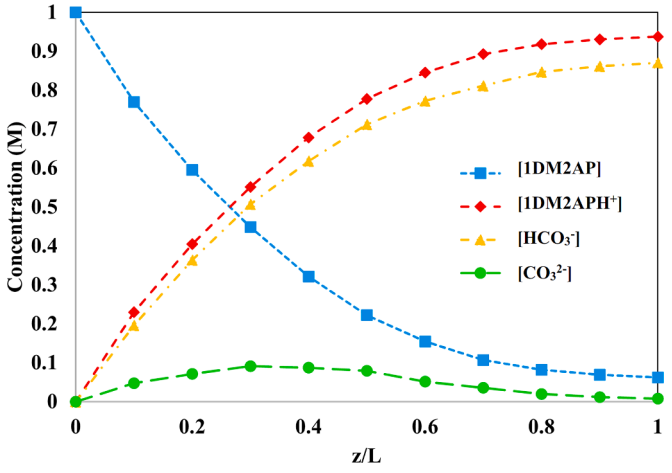

Fig. 8. The concentration profiles of chemical species in the CO_2+H2O+1DMA2P system along the HFMC at T = 298 K, U_g = 0.1 m/s, U_l =0.05 (m/s), P = 120 kPa, $C_{absorbent}$ = 1 M and 3600 number of fibers.

5.6. Concentration profiles through the dimensionless length of HFMC

The axial dimensionless concentration profiles (C/C_0) of CO_2 and 1DMA2P in the shell and tube sides of the membrane contactor for the non-wetting mode are illustrated in Fig. 7. The initial absorbent concentration is 2 M. According to demonstrated configuration in Fig. 1, the feed gas mixture enters the shell side from the bottom section of the contactor (z = 1), where the concentration of CO_2 is assumed to be maximum, at z/L = 1. Also the 1DMA2P solution enters the tube side from the top section of the contactor (z = L). The main mechanisms of mass transfer in the HFMC are diffusion and convection. Due to concentration gradient between the shell and membrane sides, the CO_2 molecules diffuse through the membrane pores and then absorb into the amine solvent. Based on reported results in Fig. 7, the final concentration of CO_2 in the 1DMA2P solution is approximately 33% of its initial value. Also as can be seen, the reduction of concentration at the entrance of contactor is sharper which is related to higher mass transfer driving force. Also, because of chemical reaction between 1DMA2P and CO_2 molecules, the concentration of 1DMA2P decreases in the module. The outlet concentration of 1DMA2P is 6% of its initial concentration. This large decrease of 1DMA2P concentration is related to high reaction rate, solubility and capacity of 1DMA2P solvent.

The concentration profiles of chemical species in the CO_2+H2O+1DMA2P system through the dimensionless length of HFMC are illustrated in Fig. 8. It is reasonable that the free concentration of 1DMA2P decreases continuously through the dimensionless length of HFMC due to chemical reaction of CO_2 with 1DMA2P solution and the occurrence of 1DMA2P protonation. Also based on this figure, the protonated concentration ($1DMA2PH^+$) and the concentration of HCO_3^- increases as the CO_2 molecules react with 1DMA2P. The concentration profile of CO_3^{2-} represents different trend respect to other species. The CO_3^{2-} concentration enhances at the entrance section of HFMC, and reaches a maximum value at 0.3 of z/L. This increasing trend is related to excess amount of 1DMA2P molecules at the entrance section of HFMC and high pH value. But in the following, because of converting CO_3^{2} to HCO_3 via the reverse reaction of the bicarbonate ion dissociation, the CO_3^{2-} concentration reduces.

5.7. Comparison of operational modes

The operational mode has a great impact on the amount of CO_2 absorption, since it significantly influences the mass transfer rate. The variations of CO_2 absorption as a function of main operating conditions for co- and counter-current operational modes are compared in Fig. 9. As presented in this figure, at different operational conditions, the counter-current flow mode generally has a superior performance with respect to co-current flow, since in the counter-current flow, higher driving force for CO_2 transfer from the gas phase to the liquid phase is available through the length of HFMC. According to predicted results in Fig. 9-a and b, the effect of liquid and gas velocities on the percentage of CO_2 absorption in the counter-current operational mode is more significant

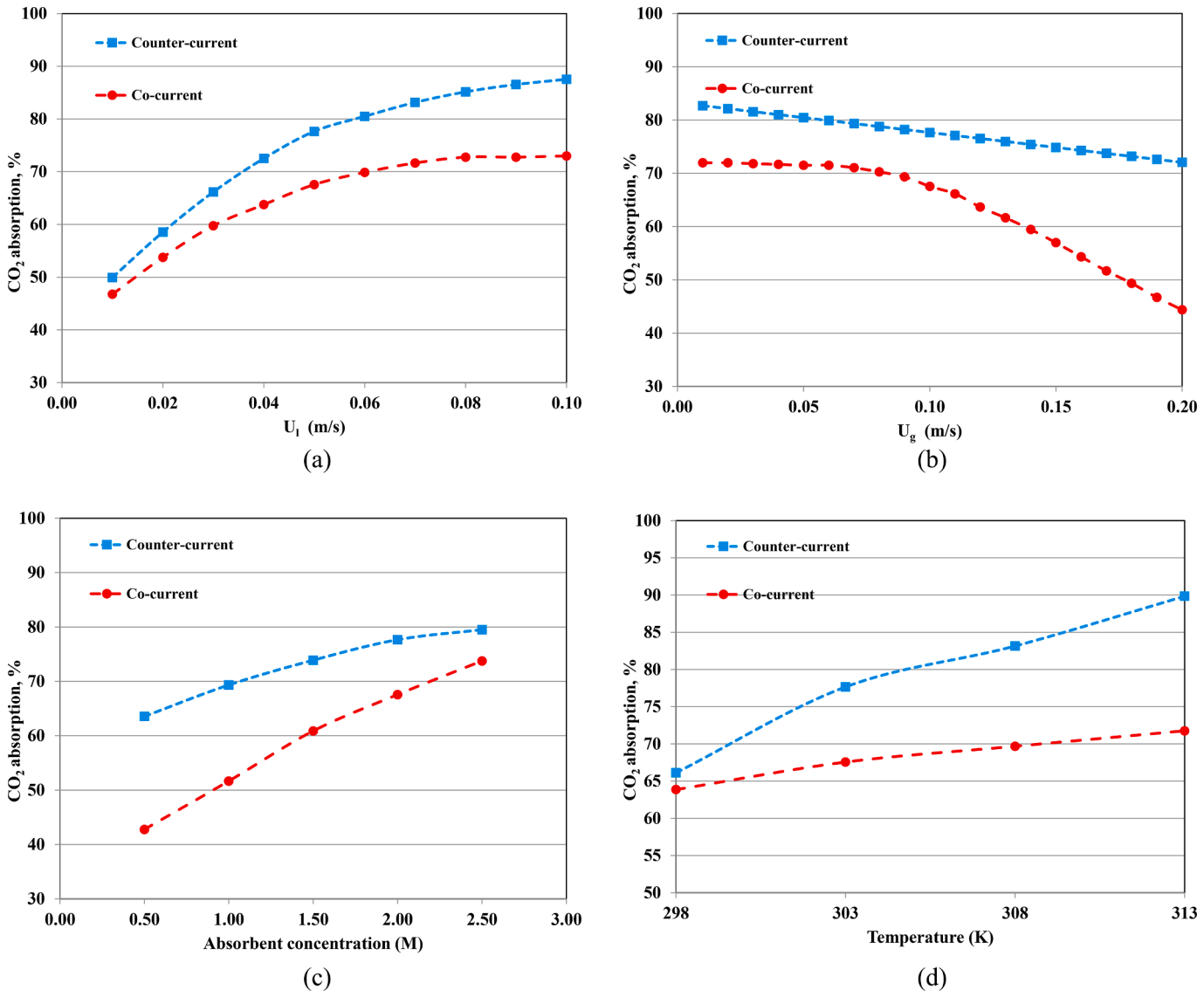

Fig. 9. Comparison of co- and counter-current operational modes in the case of non-wetting mode at (a) T = 298 K, U_g = 0.1 m/s, P = 120 kPa, $C_{absorbent}$ = 1 M and 3600 number of fibers, (b) T = 298 K, U_l = 0.05 m/s, P = 120 kPa, $C_{absorbent}$ = 1 M and 3600 number of fibers, (c) T = 298 K, U_l = 0.05 m/s, U_g = 0.1 m/s, P = 120 kPa, and 3600 number of fibers, (d) U_g = 0.1 m/s, U_l = 0.05 m/s, P = 120 kPa, $C_{absorbent}$ = 1 M and 3600 number of fibers.

Table 2
Kinetic parameters of different amines used in this study.

Amine	K ($m^3kmol^{-1}s^{-1}$)	Reference
MEA	$5.127 \times 10^8 \exp\left[\frac{-3373.8}{T}\right]$	[32]
DEA	$1.24 \times 10^6 \exp\left[\frac{-1701}{T}\right]$	[22]
TEA	$1.01 \times 10^7 \exp\left[\frac{-4415}{T}\right]$	[33]
MDEA	$1.34 \times 10^9 \exp\left[\frac{-5771}{T}\right]$	[33]
DEAB	$4.01 \times 10^{13} \exp\left[\frac{-7527.7}{T}\right]$	[31]

than co-current mode. Also, by investigation of Fig. 9-a and b, it can be observed that the performance difference between co- and counter-current operational modes at higher values of liquid and gas velocities is more significant. Fig. 9-c illustrates the effect of 1DMA2P concentration on the CO_2 removal in different operational modes. The results indicate that at higher absorbent concentrations, the performance of co- and counter-current operational modes are close to each other which can be related to availability of excess 1DMA2P molecules which compensate the lower mass transfer deriving force in the case of co-current mode. Also, the positive effect of increasing liquid temperature on the CO_2 absorption in the counter-current operational mode is more severe than co-current mode, because increasing the liquid temperature enhances the reactions rate and reduces mass transfer resistance in the liquid phase, therefore due to higher concentration gradient in the counter-current operational mode, more CO_2 molecules will absorb in this case.

5.8. Performance analysis of different solvents

The kinetic parameters of different amines are reported in Table 2. The performance of different amine solvents for the CO_2 removal is compared in Fig. 10 and Table 3. The dimensionless concentrations of different amine solvents across the membrane are shown in Fig. 10. The results indicated that among different amine solutions, PZ, MEA and DEAB are the best absorbents for CO_2 capture and 1DMA2P is in the next rank of best absorbents. Also DEA and MDEA are the weakest absorbents

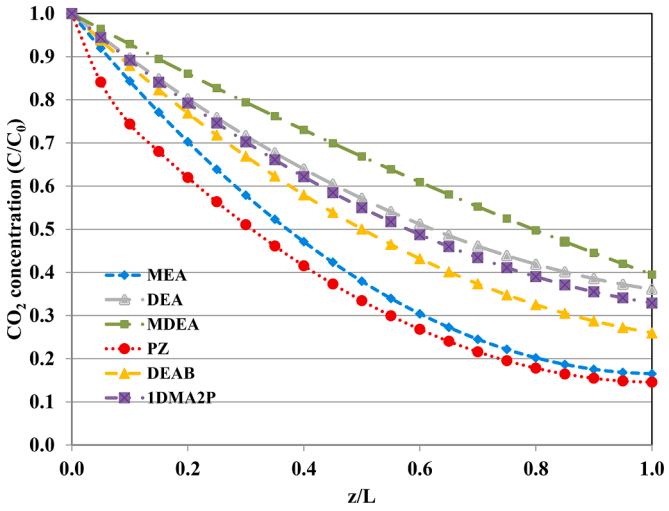

Fig. 10. CO_2 concentration profile for various absorbents along the HFMC at T = 298 K, U_g = 0.2 m/s, U_l =0.01 (m/s), P = 120 kPa and $C_{absorbent}$ = 1 M.

Table 3
Comparison of different amines in terms of main determinative parameters [8, 30,31].

Amine	Absorption heat (ΔH_a, kJ/mol)	Second order reaction constant at 298 K (k_{R-1}, m^3/ kmol s)	Equilibrium CO_2 solubility at 2 M, 313 K, 101 kPa for CO_2 partial pressure (mol CO_2/mol amine)	Percentage removal of CO_2 from CO_2/N_2 gas mixture (20%/ 80%) using HFMC at P = 120 kPa, $C_{absorbent}$ = 1 M U_g = 0.2 m/s and U_l =0.01 (m/s).
MEA	-84.3	5939	0.676	83.5%
DEA	-66.9	576	0.727	63.9%
MDEA	-54.6	12	0.805	60.5%
PZ	-70	65000	1.25	85.4%
DEAB	-41.4	429	0.99	74.0%
1DMA2P	-31.67	23	0.913	67.1%

among the considered solvents for CO_2 absorption. For selecting the efficient amine solvent, the performance of the amine across both the absorption and desorption processes should be considered. The main determinative parameters to investigate the amine performance are equilibrium CO_2 solubility, absorption reaction rate and regeneration energy consumption. As summarized in Table 2, although the CO_2 equilibrium solubility in the 1DMA2P is lower than that in the PZ and DEAB, but in comparison with common industrial solvents such as MEA, DEA and MDEA, it represents higher CO_2 solubility. The reported results in literature represent that the second order rate constant (k_{R-2}) for 1DMA2P is smaller than that for MEA, DEA, PZ, and DEAB, but much greater than that of MDEA. The CO_2 absorption heats in aqueous MEA, DEA, MDEA, PZ, DEAB and 1DMA2P solutions are reported in Table 2. The absorption heat of CO_2 in 1DMA2P solution is lowest among these amines. In addition, the ranking of CO_2 absorption percentage for these amines can be sorted as: PZ > MEA > DEAB > 1DMA2P> DEA > MDEA. Based on these reported essential parameters, it can be concluded that 1DMA2P could be applied as one of the reactive solvent for mixing with the industrial solvents such as PZ and MEA to maximize the CO_2 removal percentage.

6. Conclusions

The CO_2 removal by novel reactive 1DMA2P solution was comprehensively studied in a HFMC under non-wetted condition. The effects of important operating parameters on the absorption performance of HFMC were evaluated at temperature of 298–313 K, solvent circulation velocity of 0.01–0.10 m/s, gas stream velocity of 0.01–0.20 m/s, 1DMA2P concentration of 0.5–2.5 M and number of fibers of 500–4000. The predicted results based on two–dimensional non–isothermal stationary model indicated that the CO_2 absorption flux improves with enhancing operating temperature, solvent circulation velocity, absorbent concentration and number of fibers, and reduces with increasing gas velocity. Because of chemical absorption reaction in the liquid phase, mass transfer resistance in this phase is lower than gas phase. Therefore, it is inferred that to improve the CO_2 removal in the HFMC, the gas velocity should be justified, since the gas phase is the controlling phase. The results indicated that due to higher driving force for CO_2 transfer, the counter-current flow mode generally has a better performance with respect to co-current flow. Comparison of different conventional and alternative amine solutions revealed that the CO_2 removal percentage of 1DMA2P is higher than that of DEA and MDEA, and is also competitive with MEA, DEAB and PZ. Due to interesting properties of 1DMA2P solvent such as appropriate mass transfer rate, fast reaction kinetics, high absorption capacity and low absorption heat, this absorbent can be applied as an alternative solvent for CO_2 removal.

Authors contributions

1- Dr. Majid Saidi
Contributions: Process modeling, analyzed data and write the paper.
2- Mr. Ebrahim Balaghi Inaloob
Contributions: Analyzed data, process modeling

Declaration of Competing Interest

The authors declare that they have no conflict of interest.

References

[1] U. Ahmed, C. Kim, U. Zahid, C.-J. Lee, C. Han, Integration of IGCC and methane reforming process for power generation with CO2 capture, Chem. Eng. Process. 111 (2017) 14–24.
[2] J. Hu, X. Yang, J. Yu, G. Dai, Carbon dioxide (CO2) absorption and interfacial mass transfer across vertically confined free liquid film-a numerical investigation, Chem. Eng. Process. 111 (2017) 46–56.
[3] S. Zhang, Y. Lu, Y. Gu, X. Zhang, J. Sun, Z. Tang, The process intensification of CO2 absorption in honeycomb fractal reactor fabricated by 3D printer, Chem. Eng. Process. - Process Intensif. 132 (2018) 42–47.
[4] W. Jiao, P. Yang, G. Qi, Y. Liu, Selective absorption of H2S with High CO2 concentration in mixture in a rotating packed bed, Chem. Eng. Process. - Process Intensif. 129 (2018) 142–147.
[5] Y. Liang, H. Liu, W. Rongwong, Z. Liang, R. Idem, P. Tontiwachwuthikul, Solubility, absorption heat and mass transfer studies of CO2 absorption into aqueous solution of 1-dimethylamino-2-propanol, Fuel 144 (2015) 121–129.
[6] S. Kadiwala, A.V. Rayer, A. Henni, Kinetics of carbon dioxide (CO2) with ethylenediamine, 3-amino-1-propanol in methanol and ethanol, and with 1-dimethylamino-2-propanol and 3-dimethylamino-1-propanol in water using stopped-flow technique, Chem. Eng. J. 179 (2012) 262–271.
[7] M. Afkhamipour, M. Mofarahi, C.-H. Lee, Thermodynamic modelling using e-UNIQUAC model for CO2 absorption by novel amine solutions: 1-Dimethylamino-2-propanol (1DMA2P), 3-dimethylamino-1-propanol (3DMA1P) and 4-diethylamino-2-butanol (DEAB), Fluid Phase Equilib. 473 (2018) 50–69.
[8] H. Liu, M. Xiao, Z. Liang, P. Tontiwachwuthikul, The analysis of solubility, absorption kinetics of CO2 absorption into aqueous 1-diethylamino-2-propanol solution, AIChE J. (2016) n/a-n/a.
[9] F. Cao, H. Gao, G. Gao, Z. Liang, Mass transfer performance and correlation for CO2 absorption into aqueous 1-Dimethylamino-2-propanol (1DMA2P) solution in a PTFE hollow fiber membrane contactor, Chem. Eng. Process. - Process Intensif. (2018).
[10] D. deMontigny, P. Tontiwachwuthikul, A. Chakma, Comparing the absorption performance of packed columns and membrane contactors, Ind. Eng. Chem. Res. 44 (2005) 5726–5732.
[11] H.A. Rangwala, Absorption of carbon dioxide into aqueous solutions using hollow fiber membrane contactors, J. Membr. Sci. 112 (1996) 229–240.

[12] I. Iliuta, F. Bougie, M.C. Iliuta, CO2 removal by single and mixed amines in a hollow-fiber membrane module—investigation of contactor performance, AIChE J. 61 (2015) 955–971.
[13] M. Saidi, Mathematical modeling of CO2 absorption into novel reactive DEAB solution in hollow fiber membrane contactors; kinetic and mass transfer investigation, J. Membr. Sci. 524 (2017) 186–196.
[14] M. Saidi, S. Heidarinejad, H.R. Rahimpour, M.R. Talaghat, M.R. Rahimpour, Mathematical modeling of carbon dioxide removal using amine-promoted hot potassium carbonate in a hollow fiber membrane contactor, J. Nat. Gas Sci. Eng. 18 (2014) 274–285.
[15] P. Luis, T. Van Gerven, B. Van der Bruggen, Recent developments in membrane-based technologies for CO2 capture, Prog. Energy Combust. Sci. 38 (2012) 419–448.
[16] Z. Cui, D. deMontigny, Part 7: a review of CO2 capture using hollow fiber membrane contactors, Carbon Manag. 4 (2013) 69–89.
[17] N. Hilal, A.F. Ismail, C. Wright, Membrane Fabrication, CRC Press, 2015.
[18] T.L. Donaldson, Y.N. Nguyen, Carbon dioxide reaction kinetics and transport in aqueous amine membranes, Ind. Eng. Chem. Fundam. 19 (1980) 260–266.
[19] R.L. Kent, B. Elsenberg, Better data for amine treating, Hydrocarbon Process. 55 (1976) 87–90.
[20] D.M. Austgen, G.T. Rochelle, X. Peng, C.C. Chen, Model of vapor-liquid equilibria for aqueous acid gas-alkanolamine systems using the electrolyte-NRTL equation, Ind. Eng. Chem. Res. 28 (1989) 1060–1073.
[21] M.-H. Li, K.-P. Shen, Calculation of equilibrium solubility of carbon dioxide in aqueous mixtures of monoethanolamine with methyldiethanolamine, Fluid Phase Equilib. 85 (1993) 129–140.
[22] E.B. Rinker, S.S. Ashour, O.C. Sandall, Kinetics and modeling of carbon dioxide absorption into aqueous solutions of diethanolamine, Ind. Eng. Chem. Res. 35 (1996) 1107–1114.
[23] M. Afkhamipour, M. Mofarahi, Rate-based modeling and sensitivity analysis of a packed column for post-combustion CO2 capture into a novel reactive 1-dimethylamino-2-propanol (1DMA2P) solution, Int. J. Greenh. Gas Control 65 (2017) 137–148.
[24] G.F. Versteeg, W. Van Swaalj, Solubility and diffusivity of acid gases (carbon dioxide, nitrous oxide) in aqueous alkanolamine solutions, J. Chem. Eng. Data 33 (1988) 29–34.
[25] J.D. Seader, E.J. Henley, D.K. Roper, Separation Process Principles, Wiley, New York, 1998.
[26] R. Faiz, M. Al-Marzouqi, CO2 removal from natural gas at high pressure using membrane contactors: model validation and membrane parametric studies, J. Membr. Sci. 365 (2010) 232–241.
[27] S. Chapman, T. Cowling, The Mathematical Theory of Non-uniform Gases, Cambridge Math, Library, 1970.
[28] S. Nii, H. Takeuchi, Removal of CO2 and/or SO2 from gas streams by a membrane absorption method, Gas Separ. Purif. 8 (1994) 107–114.
[29] S.-p. Yan, M.-X. Fang, W.-F. Zhang, S.-Y. Wang, Z.-K. Xu, Z.-Y. Luo, K.-F. Cen, Experimental study on the separation of CO2 from flue gas using hollow fiber membrane contactors without wetting, Fuel Process. Technol. 88 (2007) 501–511.
[30] H. Liu, H. Gao, R. Idem, P. Tontiwachwuthikul, Z. Liang, Analysis of CO2 solubility and absorption heat into 1-dimethylamino-2-propanol solution, Chem. Eng. Sci. 170 (2017) 3–15.
[31] T. Sema, A. Naami, Z. Liang, R. Idem, P. Tontiwachwuthikul, H. Shi, P. Wattanaphan, A. Henni, Analysis of reaction kinetics of CO2 absorption into a novel reactive 4-diethylamino-2-butanol solvent, Chem. Eng. Sci. 81 (2012) 251–259.
[32] T. Sema, A. Naami, K. Fu, M. Edali, H. Liu, H. Shi, Z. Liang, R. Idem, P. Tontiwachwuthikul, Comprehensive mass transfer and reaction kinetics studies of CO2 absorption into aqueous solutions of blended MDEA–MEA, Chem. Eng. J. 209 (2012) 501–512.
[33] R. Littel, W.P.M. Van Swaaij, G.F. Versteeg, Kinetics of carbon dioxide with tertiary amines in aqueous solution, AIChE J. 36 (1990) 1633–1640.